Quim. Nova, Vol. 48, No. 6, 2025

Supplementary Material

METABOLIC DIVERSITY OF ZOANTHARIANS COLLECTED AT BRAZILIAN OCEANIC ISLANDS

Bianca Del B. Sahm[a,b,#], Ana C. Zanatta[b,#], Francisco da Chagas L. Pinto[c], Otília D. L. Pessoa[c], Diego V. Wilke[d], Paula C. Jimenez[e], Norberto P. Lopes[b], Tito M. C. Lotufo[f] and Letícia V. Costa-Lotufo[a,*]

[a]Laboratório de Farmacologia de Produtos Naturais Marinhos, Instituto de Ciências Biomédicas, Universidade de São Paulo, 05508-000 São Paulo – SP, Brasil

[b]Núcleo de Pesquisa em Produtos Naturais e Sintéticos, Faculdade de Ciências Farmacêuticas de Ribeirão Preto, Universidade de São Paulo, 14040-903 Ribeirão Preto – SP, Brasil

[c]Laboratório de Fitoquímica de Plantas Medicinais, Departamento de Química Orgânica e Inorgânica, Universidade Federal do Ceará, 60021-970 Fortaleza – CE, Brasil

[d]Núcleo de Pesquisa e Desenvolvimento de Medicamentos, Laboratório de Bioprospecção e Biotecnologia Marinha, Universidade Federal do Ceará, 60430-275 Fortaleza – CE, Brasil

[e]Laboratório de Bioprospecção de Organismos Marinhos, Instituto do Mar, Universidade Federal de São Paulo, 11070-100 Santos – SP, Brasil

[f]Laboratório de Biologia Recifal, Instituto de Oceanografia, Universidade de São Paulo, 05508-900 São Paulo – SP, Brasil

Received: 03/10/2025; accepted: 06/10/2025; published online: 07/22/2025

*e-mail: costalotufo@usp.br

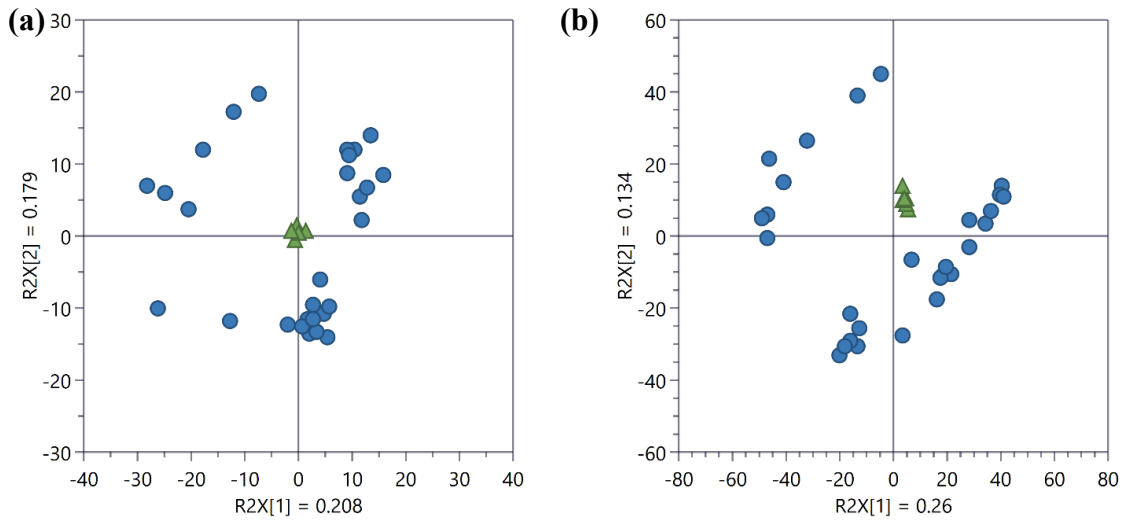

Figure 1S. *Principal component analysis (PCA) score plots assessing the quality and reproducibility of GC-MS (a) and LC-MS/MS (b) data. Zoantharian samples are represented by blue circles, while quality control (QC) samples are shown as green triangles. The tight clustering of QC samples confirms the analytical stability and reproducibility of the dataset*

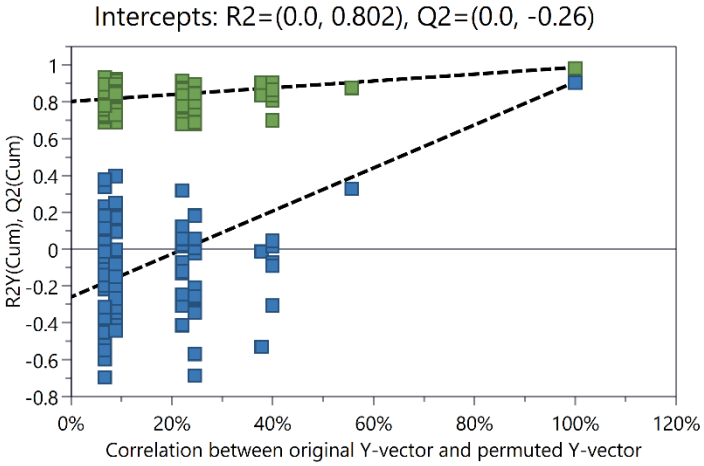

Figure 2S. *Cross-validation of the partial least squares discriminant analysis (PLS-DA) model using permutation testing. The plot shows the correlation between the original Y-vector and permuted Y-vectors, with R^2 (green) representing the goodness of fit and Q^2 (blue) indicating the predictive ability of the model. The negative Q^2 intercept and the decreasing trend of permuted Q^2 values confirm that the model is not overfitted, ensuring its reliability in discriminating metabolomic differences among zoantharian samples*

Table 1S. Decimal GPS coordinates of sampled zoantharian species at Brazilian oceanic islands in 2014 and 2015. Coordinates were obtained from Google Maps[1]

Site	*Palythoa caribaeorum*	GPS coordinates	Site	*Palythoa variabilis*	GPS coordinates	Site	*Zoanthus* spp.	GPS coordinates
				2014				
FNA	PCFN1	–3.833830, –32.400427	RA	PVAT-11	–3.859375, –33.813564	RA	ZAT-11	–3.859375, –33.813564
	PCFN2	–3.836641, –32.403201		PVAT-12	–3.859375, –33.813564		ZAT-12	–3.859375, –33.813564
	PCFN3	–3.848873, –32.441655		PVAT-13	–3.859375, –33.813564		ZAT-13	–3.859375, –33.813564
RA	PCAT31	–3.869197, –33.803175		PVAT-31	–3.869197, –33.803175		ZAT-31	–3.869197, –33.803175
	PCAT32	–3.869197, –33.803175		PVAT-32	–3.869197, –33.803175		ZAT-32	–3.869197, –33.803175
	PCAT09	–3.874145, –33.810110		PVAT-33	–3.869197, –33.803175		ZAT-33	–3.869197, –33.803175
				2015				
TR	PCTR02	–20.516732, –29.303678	SPSPA	ASPV2A	0.916369, –29.345647	TR	ZTR2B	–20.525664, –29.300016
	PCTR05	–20.494079, –29.341797		ASPV2B	0.916369, –29.345647		ZTR06	–20.516022, –29.304564
	PCTR06	–20.494079, –29.341797		ASPV2C	0.916369, –29.345647			
SPSPA	ASPC1A	0.916804, –29.345502	FNA	PVFN03	–3.834495, –32.397882			

GPS: global positioning system; PC: *Palythoa caribaeorum*; PV: *Palythoa variabilis*; Z: *Zoanthus* spp; SPSPA: Saint Peter and Saint Paul Archipelago; RA: Rocas Atoll; FNA: Fernando de Noronha Archipelago; TR: Trindade Island.

Table 2S. MZmine processing parameters for LC-MS/MS data analysis

Parameter	Setting
MS1 threshold	1.00E+03
MS2 threshold	1.00E+01
MS tolerance	20 ppm
Smoothing	yes
Chromatogram deconvolution algorithm	local minimum resolver (90%, 0.1 min, 1%, 1.00E+03, 2.00, 0.01-5 min, 4 scans)
Isotope filter	5 ppm, 0.05 min, 2
Feature alignment	10 ppm, 0.3 min, 3:1
Gap filling	20%
Filtering	Min peaks in a row: 2
Duplicate filter	yes

LC-MS/MS: liquid chromatography tandem mass spectrometry.

Table 3S. GC-MS annotation of compounds in hexane fractions of extracts from zoantharian species at each location and sampling year. Retention indices were determined experimentally and compared with literature values

n	Annotation	RI / min	RI Exp.	RI Lit.[a]	Specie	Location	Year	Class
1	2-Heptenal	5.48	954	952	PC, PV, Z	SPSPA, RA, FNA, TR	2014, 2015	aldehyde
2	2-Octenal	7.89	1056	1055	PC, PV, Z	SPSPA, RA, FNA, TR	2014, 2015	aldehyde
3	2-Nonenal	10.63	1158	1158	PC, Z	RA	2014	aldehyde
4	2-Decenal	13.43	1261	1262	PC, PV, Z	SPSPA, RA, FNA, TR	2014, 2015	aldehyde
5	2-Undecanone	14.26	1291	1291	PC, PV, Z	SPSPA, RA, FNA, TR	2014, 2015	ketone
6	2-Undecenal	16.14	1363	1361	PC, PV, Z	RA, FNA, TR	2014, 2015	aldehyde
7	Tetradecanal	22.17	1612	1614	PC, PV, Z	SPSPA, RA, FNA, TR	2014, 2015	aldehyde
8	Tetradecanol	23.73	1676	1675	PC, PV, Z	SPSPA, RA, FNA, TR	2014, 2015	alcohol
9	Pentadecanal	24.56	1713	1713	PC, PV, Z	SPSPA, RA, FNA, TR	2014, 2015	aldehyde
10	Methyl tetradecanoate (methyl myristate)	24.75	1722	1722	PC, PV, Z	SPSPA, RA, FNA, TR	2014, 2015	fatty acid methyl ester (FAME)
11	Tetradecanoic acid (myristic acid)	25.46	1755	1752	PC, PV, Z	SPSPA, RA, FNA, TR	2014, 2015	fatty acid
12	2-Hexadecanone	26.36	1797	1800	PC, PV, Z	SPSPA, RA, FNA, TR	2014, 2015	ketone
13	Hexadecanal (palmitic aldehyde)	26.74	1816	1817	PC, PV, Z	SPSPA, RA, FNA, TR	2014, 2015	aldehyde
14	6,10,14-Trimethyl-2-pentadecanone	27.23	1840	1836	PC, PV, Z	SPSPA, RA, FNA, TR	2014, 2015	ketone
15	1-Hexadecanol	28.03	1879	1880	PC, PV, Z	SPSPA, RA, FNA, TR	2014, 2015	alcohol
16	Methyl 9-hexadecenoate (methyl palmitoleate)	28.47	1900	1895	PC, PV, Z	SPSPA, RA, FNA, TR	2014, 2015	fatty acid methyl ester (FAME)

Table 3S. GC-MS annotation of compounds in hexane fractions of extracts from zoantharian species at each location and sampling year. Retention indices were determined experimentally and compared with literature values (cont.)

n	Annotation	RI / min	RI Exp.	RI Lit.[a]	Specie	Location	Year	Class
17	Heptadecanal	28.81	1917	1920	PC, PV, Z	SPSPA, RA, FNA, TR	2014, 2015	aldehyde
18	Methyl hexadecanoate (methyl palmitate)	28.93	1924	1927	PC, PV, Z	SPSPA, RA, FNA, TR	2014, 2015	fatty acid methyl ester (FAME)
19	9-Hexadecenoic acid (palmitoleic acid)	29.16	1935	1941	PC, PV, Z	SPSPA, RA, FNA, TR	2014, 2015	fatty acid
20	Hexadecanoic acid (palmitic acid)	29.57	1956	1958	PC, PV, Z	SPSPA, RA, FNA, TR	2014, 2015	fatty acid
21	Ethyl hexadecanoate (ethyl palmitate)	30.28	1993	1994	PC, PV, Z	SPSPA, RA, FNA, TR	2014, 2015	fatty acid ethyl ester (FAEE)
22	Octadecanal (stearaldehyde)	30.79	2020	2021	PC, PV, Z	SPSPA, RA, FNA, TR	2014, 2015	aldehyde
23	9-Octadecenol	31.5	2058	2060	PC, PV, Z	SPSPA, RA, FNA, TR	2014, 2015	alcohol
24	Methyl 9,12,15-octadecatrienoate (methyl linolenate)	31.76	2072	2073	PC, PV, Z	SPSPA, RA, FNA, TR	2014, 2015	fatty acid methyl ester (FAME)
25	1-Octadecanol	31.97	2083	2082	PC, PV, Z	SPSPA, RA, FNA, TR	2014, 2015	alcohol
26	Methyl 9,12-octadecadienoate (methyl linoleate)	32.09	2089	2092	PC, PV, Z	SPSPA, RA, FNA, TR	2014, 2015	fatty acid methyl ester (FAME)
27	3,7,11,15-Tetramethyl-2-hexadecenol (phytol)	32.39	2106	2105	PC, PV, Z	SPSPA, RA, FNA, TR	2014, 2015	diterpenoid alcohol
28	Methyl octadecanoate (methyl stearate)	32.72	2124	2128	PC, PV, Z	SPSPA, RA, FNA, TR	2014, 2015	fatty acid methyl ester (FAME)

Table 3S. GC-MS annotation of compounds in hexane fractions of extracts from zoantharian species at each location and sampling year. Retention indices were determined experimentally and compared with literature values (cont.)

n	Annotation	RI / min	RI Exp.	RI Lit.[a]	Specie	Location	Year	Class
29	9-Octadecenoic acid (oleic acid)	32.87	2132	2131	PC, PV, Z	SPSPA, RA, FNA, TR	2014, 2015	fatty acid
30	Ethyl 9,12,15-octadecatrienoate (ethyl linolenate)	32.96	2137	2135	PC, PV, Z	SPSPA, RA, FNA, TR	2014, 2015	fatty acid ethyl ester (FAEE)
31	Octadecanoic acid (stearic acid)	33.12	2146	2143	PC, PV, Z	RA, FNA, TR	2014, 2015	fatty acid
32	5,8,11,14-Eicosatetraenoic acid (arachidonic acid)	35.67	2292	-	PC, PV, Z	SPSPA, RA, FNA, TR	2014, 2015	fatty acid
33	Methyl eicosanoate (methyl arachidate)	36.21	2325	2324	PC, PV, Z	SPSPA, RA, FNA, TR	2014, 2015	fatty acid methyl ester (FAME)
34	Octadecanamide	36.66	2352	2349	PC, PV, Z	SPSPA, RA, FNA, TR	2014, 2015	fatty acid amide
35	Hexadecyl octanoate	40.13	2572	2576	PC, PV, Z	SPSPA, RA, FNA, TR	2014, 2015	fatty acid ester
36	Tetradecyl tetradecanoate (myristyl myristate)	45.67	2964	–	PC, PV, Z	SPSPA, RA, FNA, TR	2014, 2015	wax ester (saturated)
37	Cholesta-4,6-dien-3-ol	46.85	3055	–	PC, PV, Z	SPSPA, RA, FNA, TR	2014, 2015	sterol
38	Cholesta-5,22-dien-3-ol	46.96	3064	3070	PC, PV, Z	SPSPA, RA, FNA, TR	2014, 2015	sterol
39	Cholesterol	47.49	3106	3098	PC, PV, Z	SPSPA, RA, FNA, TR	2014, 2015	sterol
40	Ergosta-5,22-dien-3-ol	48.03	3148	–	PC, PV, Z	SPSPA, RA, FNA, TR	2014, 2015	sterol
41	Tetradecyl hexadecanoate (myristyl palmitate)	48.22	3164	–	PC, PV, Z	SPSPA, RA, FNA, TR	2014, 2015	wax ester (saturated)
42	24-Methylene cholesterol	48.75	3207	–	PC, PV, Z	SPSPA, RA, FNA, TR	2014, 2015	sterol

Table 3S. GC-MS annotation of compounds in hexane fractions of extracts from zoantharian species at each location and sampling year. Retention indices were determined experimentally and compared with literature values (cont.)

n	Annotation	RI / min	RI Exp.	RI Lit.[a]	Specie	Location	Year	Class
43	Campesterol	48.84	3214	–	PC, PV, Z	SPSPA, RA, FNA, TR	2014, 2015	sterol
44	Ergostanol	48.98	3226	–	PC, PV, Z	SPSPA, RA, FNA, TR	2014, 2015	sterol
45	*epi*-5β-Campestanol	49.76	3291	3284	PC, PV, Z	SPSPA, RA, FNA, TR	2014, 2015	sterol
46	Stigmastanol	49.9	3325	3317	PC, PV, Z	SPSPA, RA, FNA, TR	2014, 2015	sterol
47	Hexadecyl hexadecanoate (palmityl palmitate)	50.63	3365	–	PC, PV, Z	SPSPA, RA, FNA, TR	2014, 2015	wax ester (saturated)
48	7-Oxocholesterol	51.12	3407	3410	PC, PV, Z	SPSPA, RA, FNA, TR	2014, 2015	sterol
49	Gorgostenol	51.51	3441	–	PC, PV, Z	SPSPA, RA, FNA, TR	2014, 2015	sterol
50	Hexadecyl 9,12-octadecadienoate (palmityl linolenate)	52.29	3510	3515	PC, PV, Z	SPSPA, RA, FNA, TR	2014, 2015	wax ester (unsaturated)
51	Hexadecyl octadecanoate (palmityl stearate)	52.88	3563	–	PC, PV, Z	SPSPA, RA, FNA, TR	2014, 2015	wax ester (saturated)
52	Hexadecyl eicosanoate (palmityl arachidate)	55.36	3761	–	PC, PV, Z	SPSPA, RA, FNA, TR	2014, 2015	wax ester (saturated)
53	Octadecyl eicosanoate (stearyl arachidate)	58.68	3962	–	PC, PV, Z	SPSPA, RA, FNA, TR	2014, 2015	wax ester (saturated)

[a]For compounds without retention index (RI) values available in the literature, the identification was based on spectral similarity matching; GC-MS: gas chromatography coupled with mass spectrometry; RI: retention indice; RI Exp.: retention indice determined experimentally; RI Lit.; retention indice from the literature; PC: *Palythoa caribaeorum*; PV: *Palythoa variabilis*; Z: *Zoanthus* spp.; SPSPA: Saint Peter and Saint Paul Archipelago; RA: Rocas Atoll; FNA: Fernando de Noronha Archipelago; TR: Trindade Island.

Table 4S. LC-MS/MS-based annotation of major metabolites in methanolic extracts from zoantharian species. Annotations were performed based on precursor mass values, cross-referenced with GNPS spectral libraries[2] and *in silico* predictions using SIRIUS[3]

n	Annotation	RT / min	Adduct	*m/z*	Molecular formula	Error / ppm	Specie	Location	Year
Mycosporine-like amino acids									
1[a]	Palythene	1.35	$[M + H]^+$	285.1447	$C_{13}H_{20}N_2O_5$	–1.2	PC, PV	SPSPA, RA, FNA, TR	2014, 2015
Pyrazine alkaloids									
2	Palythazine	1.74	$[M + H]^+$	253.1194	$C_{12}H_{16}N_2O_4$	2.2	PC, PV	SPSPA, RA, FNA, TR	2014, 2015
Ecdysteroids									
3	Dihydroxyecdysone	4.43	$[M + H]^+$	497.311	$C_{27}H_{44}O_8$	–0.9	PC, PV, Z	RA, FNA	2014, 2015
4	Didehydro-heptahydroxyergostenone	5.46	$[M + H]^+$	509.3093	$C_{28}H_{44}O_8$	–4.2	PC, PV, Z	RA, FNA	2014, 2015
5	Dehydro-hydroxyecdysone	5.82	$[M + H]^+$	479.3001	$C_{27}H_{42}O_7$	–1.6	PC, PV, Z	RA, FNA, TR	2014, 2015
6[a]	Hydroxyecdysone	5.93	$[M + H]^+$	481.3159	$C_{27}H_{44}O_7$	–1.3	PC, PV, Z	SPSPA, RA, FNA, TR	2014, 2015
7	Dehydroecdysone	5.97	$[M + H]^+$	463.3065	$C_{27}H_{42}O_6$	1.2	PC, PV, Z	SPSPA, RA, FNA, TR	2014, 2015
8	Dihydroxymethylecdysone	6.87	$[M + H]^+$	511.3279	$C_{28}H_{46}O_8$	1.6	PV, Z	RA, FNA	2014, 2015
9	Hexahydroxyergostadienone	7.03	$[M + H]^+$	493.3153	$C_{28}H_{44}O_7$	–2.5	PC, PV, Z	SPSPA, RA, FNA, TR	2014, 2015
10	Didehydro-heptahydroxyergostenone	7.13	$[M + H]^+$	509.3111	$C_{28}H_{44}O_8$	–0.7	PV, Z	RA, FNA	2014, 2015
11	Acetyl-hydroxyecdysone	7.58	$[M + H]^+$	523.3257	$C_{29}H_{46}O_8$	–2.7	PC, PV, Z	SPSPA, RA, FNA, TR	2014, 2015
12	Ecdysone	7.68	$[M + H]^+$	465.3198	$C_{27}H_{44}O_6$	–3.9	PC, PV, Z	SPSPA, RA, FNA, TR	2014, 2015
13	Deoxy-dehydro-ecdysone	7.71	$[M + H]^+$	447.3083	$C_{27}H_{42}O_5$	–6.1	PC, PV, Z	RA, FNA	2014, 2015
14[a]	Hydroxyecdysone	7.85	$[M + H]^+$	481.3168	$C_{27}H_{44}O_7$	0.6	PC, PV, Z	SPSPA, RA, FNA, TR	2014, 2015
15	Dehydroecdysone	7.87	$[M + H]^+$	463.3046	$C_{27}H_{42}O_6$	–2.9	PV, Z	RA, FNA	2014, 2015
16	Oxo-hydroxyecdysone	8.06	$[M + H]^+$	479.301	$C_{27}H_{42}O_7$	0.3	PC, PV, Z	RA, FNA	2014, 2015
17	Hexahydroxyergostadienone	8.2	$[M + H]^+$	493.3155	$C_{28}H_{44}O_7$	–2.1	PC, PV, Z	RA, FNA, TR	2014/2015
18	Ecdysone	8.79	$[M + H]^+$	465.3221	$C_{27}H_{44}O_6$	1	PV, Z	RA, FNA	2014, 2015
19	Methyl-hydroxyecdysone	8.8	$[M + H]^+$	495.3286	$C_{28}H_{46}O_7$	–7.2	PC, PV, Z	RA, FNA, TR	2014, 2015
20	Pentahydroxyergostadienone	8.96	$[M + H]^+$	477.3204	$C_{28}H_{44}O_6$	–2.5	PV, Z	RA, FNA, TR	2014, 2015

Table 4S. LC-MS/MS-based annotation of major metabolites in methanolic extracts from zoantharian species. Annotations were performed based on precursor mass values, cross-referenced with GNPS spectral libraries[2] and *in silico* predictions using SIRIUS[3] (cont.)

n	Annotation	RT / min	Adduct	*m/z*	Molecular formula	Error / ppm	Specie	Location	Year
Ecdysteroids									
21	Ecdysone	9.74	$[M + H]^+$	465.3217	$C_{27}H_{44}O_6$	0.1	PC, PV, Z	RA, FNA	2014, 2015
22	Acetyl-hydroxyecdysone	9.97	$[M + H]^+$	523.3282	$C_{29}H_{46}O_8$	2.1	PV, Z	RA	2014
23	Pentahydroxyergostadienone	10.11	$[M + H]^+$	477.3199	$C_{28}H_{44}O_6$	–3.6	PV, Z	RA, FNA	2014, 2015
Zoanthids alkaloids									
24	Norzoanthamine	5.48	$[M + H]^+$	482.2915	$C_{29}H_{39}NO_5$	1.7	PC, PV, Z	SPSPA, RA, FNA, TR	2014, 2015
25	Hydroxynorzoanthamine	5.74	$[M + H]^+$	498.2823	$C_{29}H_{39}NO_6$	–6.6	PC, PV, Z	SPSPA, RA, FNA, TR	2014, 2015
26	Acetylnorzoanthamine	6.32	$[M + H]^+$	540.2935	$C_{31}H_{41}NO_7$	–4.9	PC, PV, Z	RA, FNA, TR	2015
27	Acetylzoanthamine	6.84	$[M + H]^+$	554.3134	$C_{32}H_{43}NO_7$	2.9	PC, Z	FNA, TR	2015
28	Zoanthenamine	11.35	$[M + H]^+$	510.2833	$C_{30}H_{39}NO_6$	–4.4	PC, Z	TR	2015
29	Oxonorzoanthamine	13.94	$[M + H]^+$	496.2687	$C_{29}H_{37}NO_6$	–2.4	PC, PV, Z	SPSPA, RA, FNA, TR	2014, 2015
30	Zoanthenamine	14.41	$[M + H]^+$	510.2837	$C_{30}H_{39}NO_6$	–3.7	PC, PV, Z	SPSPA, RA, FNA, TR	2014, 2015
Glycerophospholipids									
31[a]	LPE 16:1	17.79	$[M + H]^+$	452.278	$C_{21}H_{42}NO_7P$	0.6	PC, PV, Z	SPSPA, RA, FNA, TR	2014, 2015
32	LPE 20:3	18.67	$[M + H]^+$	504.3084	$C_{25}H_{46}NO_7P$	–1.2	PC, PV, Z	SPSPA, RA, FNA, TR	2014, 2015
33	LPE 17:1	18.93	$[M + H]^+$	466.2929	$C_{22}H_{44}NO_7P$	–1	PC, PV, Z	SPSPA, RA, FNA, TR	2014, 2015
34[a]	LPC 16:0	18.95	$[M + H]^+$	496.3405	$C_{24}H_{50}NO_7P$	0.4	PC, PV, Z	SPSPA, RA, FNA, TR	2014, 2015
35	LPE 19:0	18.95	$[M + H]^+$	496.3379	$C_{24}H_{50}NO_7P$	–4.9	PC, PV, Z	SPSPA, RA, FNA, TR	2014, 2015
36[a]	LPC 17:1	19.67	$[M + H]^+$	508.3419	$C_{25}H_{50}NO_7P$	3.1	PC, PV	SPSPA, RA, FNA, TR	2014, 2015
37[a]	LPE 18:1	20.38	$[M + H]^+$	480.3104	$C_{23}H_{46}NO_7P$	2.9	PC, PV, Z	SPSPA, RA, FNA, TR	2014, 2015
38[a]	LPC 18:0	22.06	$[M + H]^+$	524.3698	$C_{26}H_{55}NO_7P$	–3.5	PC, PV, Z	SPSPA, RA, FNA, TR	2014, 2015

Table 4S. LC-MS/MS-based annotation of major metabolites in methanolic extracts from zoantharian species. Annotations were performed based on precursor mass values, cross-referenced with GNPS spectral libraries[2] and *in silico* predictions using SIRIUS[3] (cont.)

n	Annotation	RT / min	Adduct	*m/z*	Molecular formula	Error / ppm	Specie	Location	Year
Glycosyldiacylglycerols									
39[a]	MGDG 32:4	30.34	$[M + NH_4]^+$	740.5323	$C_{41}H_{70}O_{10}$	1.4	PC, PV, Z	SPSPA, RA, FNA, TR	2014, 2015
40[a]	SQDG 30:0	31.22	$[M + NH_4]^+$	784.526	$C_{39}H_{74}O_{12}S$	1.9	Z	RA, TR	2014, 2015
41[a]	MGDG 32:3	31.3	$[M + NH_4]^+$	742.5446	$C_{41}H_{72}O_{10}$	–3.1	PC, PV, Z	SPSPA, RA, FNA, TR	2014, 2015
42[a]	MGDG 30:1	31.89	$[M + NH_4]^+$	718.546	$C_{39}H_{72}O_{10}$	–1	PC, PV, Z	SPSPA, RA, FNA, TR	2014, 2015
43	MGDG 34:3	32.32	$[M + NH_4]^+$	770.5778	$C_{43}H_{76}O_{10}$	–0.6	PC, PV, Z	SPSPA, RA, FNA, TR	2014, 2015
44	MGDG 30:0	33.24	$[M + NH_4]^+$	720.5609	$C_{39}H_{74}O_{10}$	–2.3	PC, PV, Z	SPSPA, RA, FNA, TR	2014, 2015
45	MGDG 32:1	33.4	$[M + NH_4]^+$	746.5761	$C_{41}H_{76}O_{10}$	–2.8	PC, PV, Z	SPSPA, RA, FNA, TR	2014, 2015
46	MGDG 34:2	33.61	$[M + NH_4]^+$	772.592	$C_{43}H_{78}O_{10}$	–2.4	PC, PV, Z	SPSPA, RA, FNA, TR	2014, 2015
Ceramides									
47	palyosulfonoceramide B	25.79	$[M + H]^+$	659.5381	$C_{37}H_{74}N_2O_5S$	–2.4	Z	RA	2014
48	Cer 34:2;O3	32.12	$[M + H]^+$	552.4956	$C_{34}H_{65}NO_4$	–6.5	PC, PV, Z	SPSPA, RA, FNA, TR	2014, 2015
49	Cer 34:2;O2	33.33	$[M + H]^+$	536.503	$C_{34}H_{65}NO_3$	–2.4	PC, PV, Z	SPSPA, RA, FNA, TR	2014, 2015
50[a]	Cer 34:1;O2	34.86	$[M + H]^+$	538.5181	$C_{34}H_{67}NO_3$	–3.4	PC, PV, Z	SPSPA, RA, FNA, TR	2014, 2015

[a]MS/MS mirror plots are provided in Figures 3S-7S; LC-MS/MS: liquid chromatography tandem mass spectrometry; PC: *Palythoa caribaeorum*; PV: *Palythoa variabilis*; Z: *Zoanthus* spp.; SPSPA: Saint Peter and Saint Paul Archipelago; RA: Rocas Atoll; FNA: Fernando de Noronha Archipelago; TR: Trindade Island.

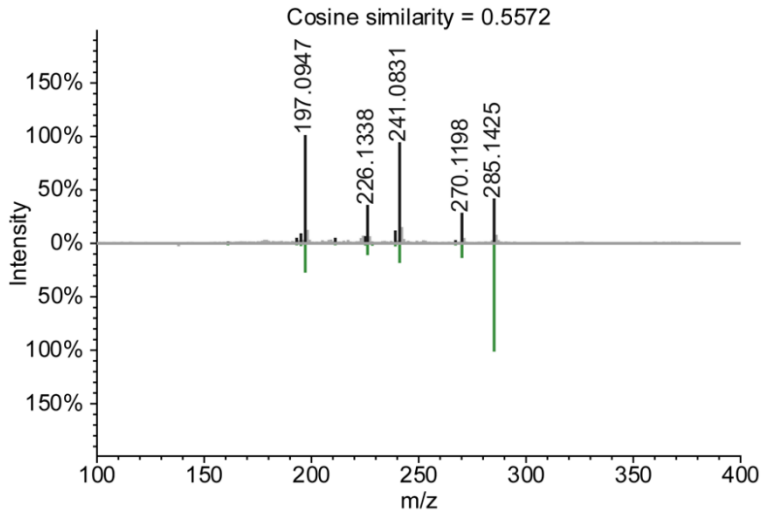

Figure 3S. *MS/MS spectral match for palythene (**1**) with GNPS spectral library (CCMSLIB00010013013,[4] cosine similarity = 0.5572). Matching fragment ions are highlighted in black (experimental, top) and green (library, bottom)*

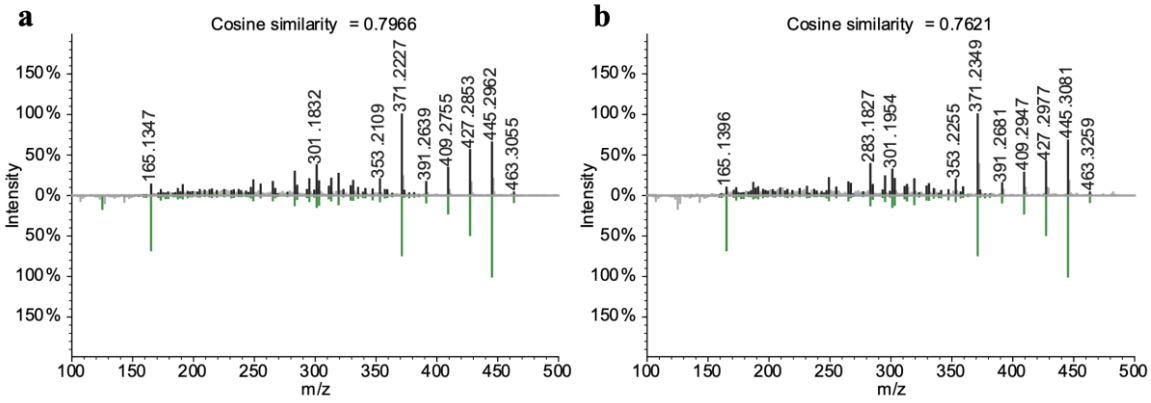

Figure 4S. *MS/MS spectral match for ecdysteroids with GNPS spectral library: (a) Hydroxyecdysone (**6**) (CCMSLIB00011427929,[5] cosine similarity = 0.7966); (b) hydroxyecdysone (**14**) (CCMSLIB00011427929,[6] cosine similarity = 0.7621). Matching fragment ions are highlighted in black (experimental, top) and green (library, bottom)*

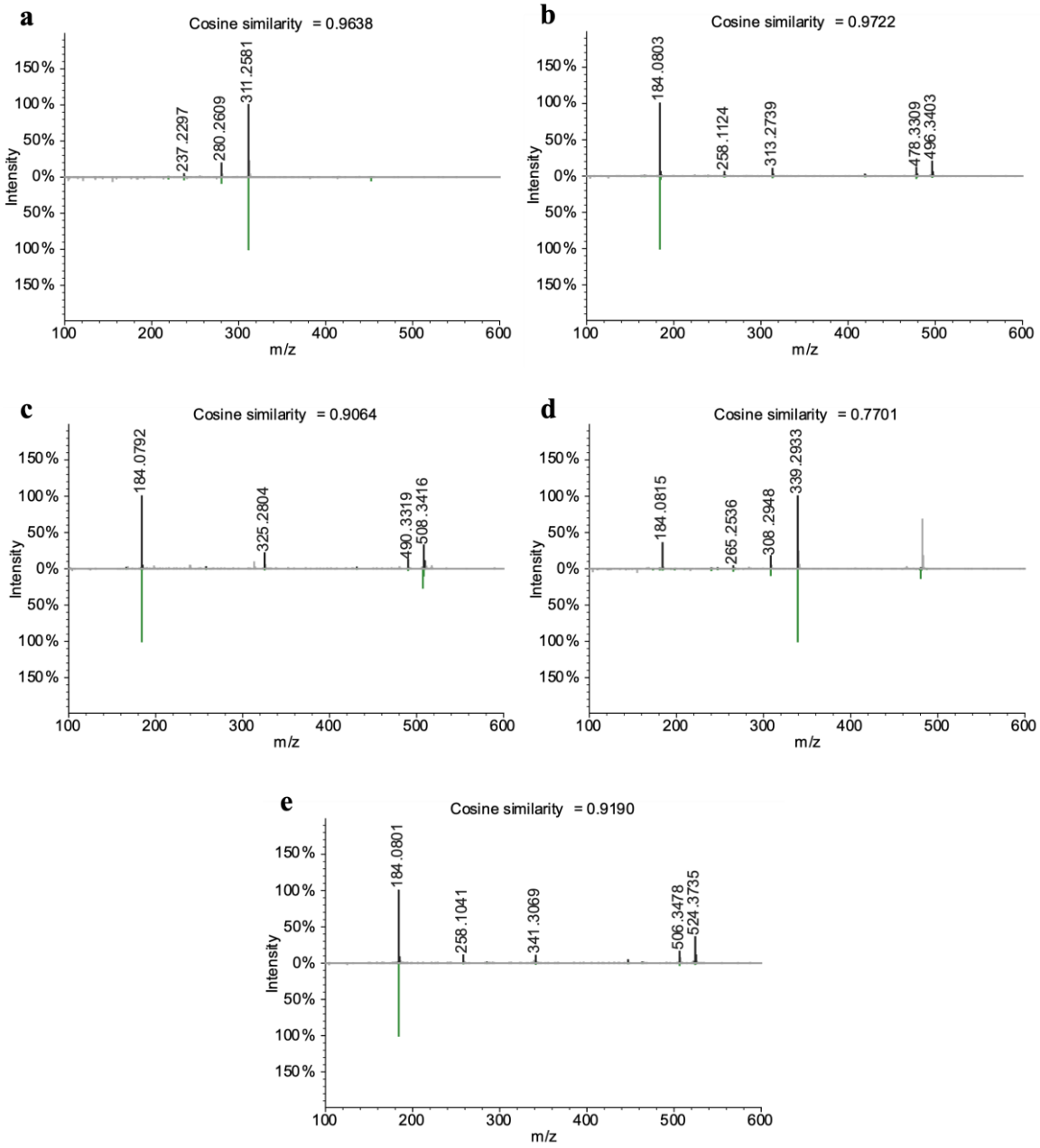

Figure 5S. *MS/MS spectral match for glycerophospholipids with GNPS spectral library: (a) LPE 16:1 (**31**) (CCMSLIB00010086490,[7] cosine similarity = 0.9638); (b) LPC 16:0 (**34**) (CCMSLIB00010063486,[8] cosine similarity = 0.9722); (c) LPC 17:1 (**36**) (CCMSLIB00010058873,[9] cosine similarity = 0.9064); (d) LPE 18:1 (**37**) (CCMSLIB00010091229,[10] cosine similarity = 0.7701); (e) LPC 18:0 (**38**) (CCMSLIB00010064591,[11] cosine similarity = 0.9190). Matching fragment ions are highlighted in black (experimental, top) and green (library, bottom)*

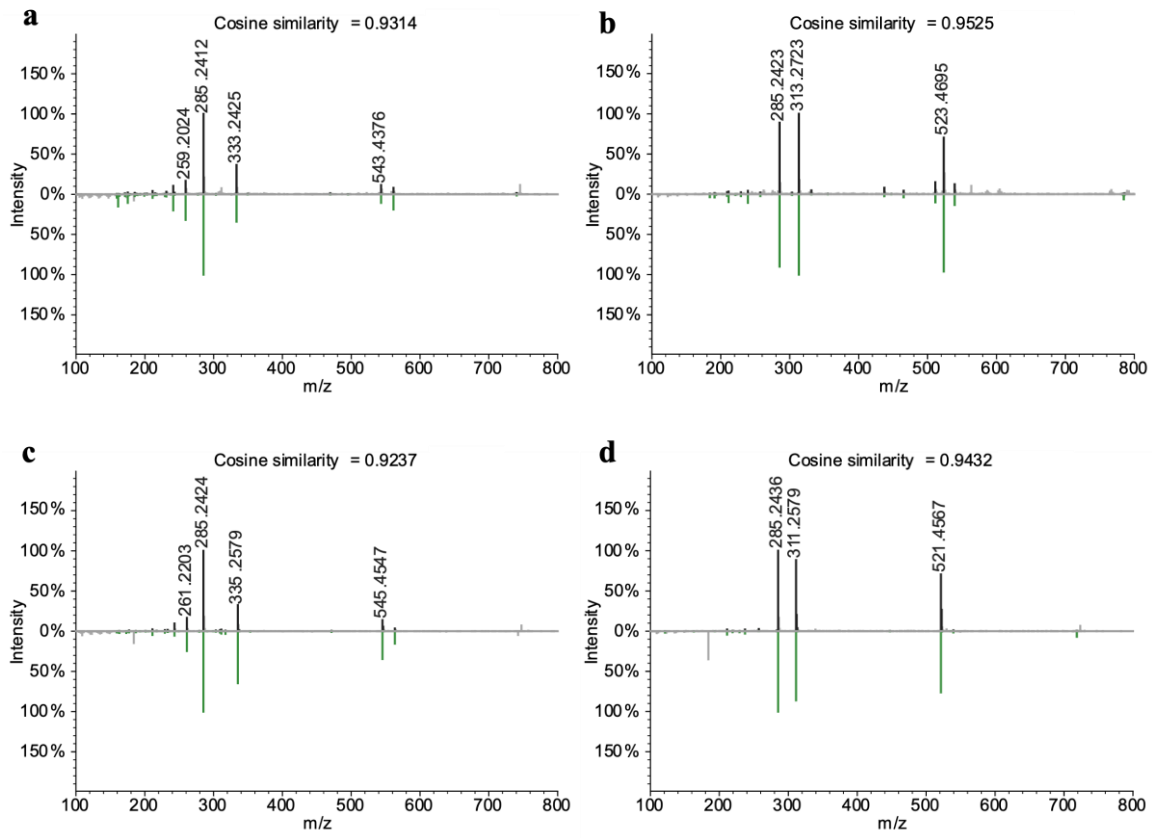

Figure 6S. *MS/MS spectral match for glycosyldiacylglycerols with GNPS spectral library: (a) MGDG 32:4 (**39**) (CCMSLIB00006678246,[12] cosine similarity = 0.9314); (b) SQDG 30:0 (**40**) (CCMSLIB00010057661,[13] cosine similarity = 0.9525); (c) MGDG 32:3 (**41**) (CCMSLIB00006678245,[14] cosine similarity = 0.9237); (d) MGDG 30:1 (**42**) (CCMSLIB00006678247,[15] cosine similarity = 0.9432). Matching fragment ions are highlighted in black (experimental, top) and green (library, bottom)*

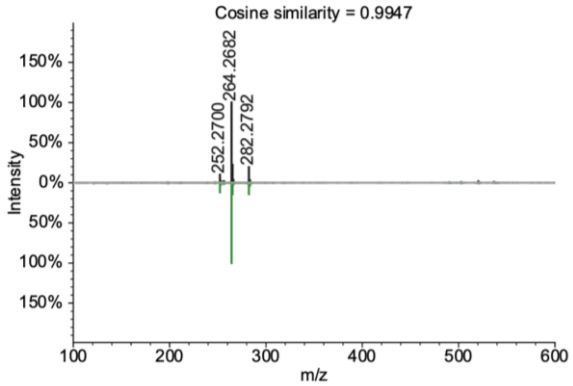

Figure 7S. *MS/MS spectral match for Cer 34:1;O2 (**50**) with GNPS spectral library (CCMSLIB00010013013,[16] cosine similarity = 0.9947). Matching fragment ions are highlighted in black (experimental, top) and green (library, bottom)*

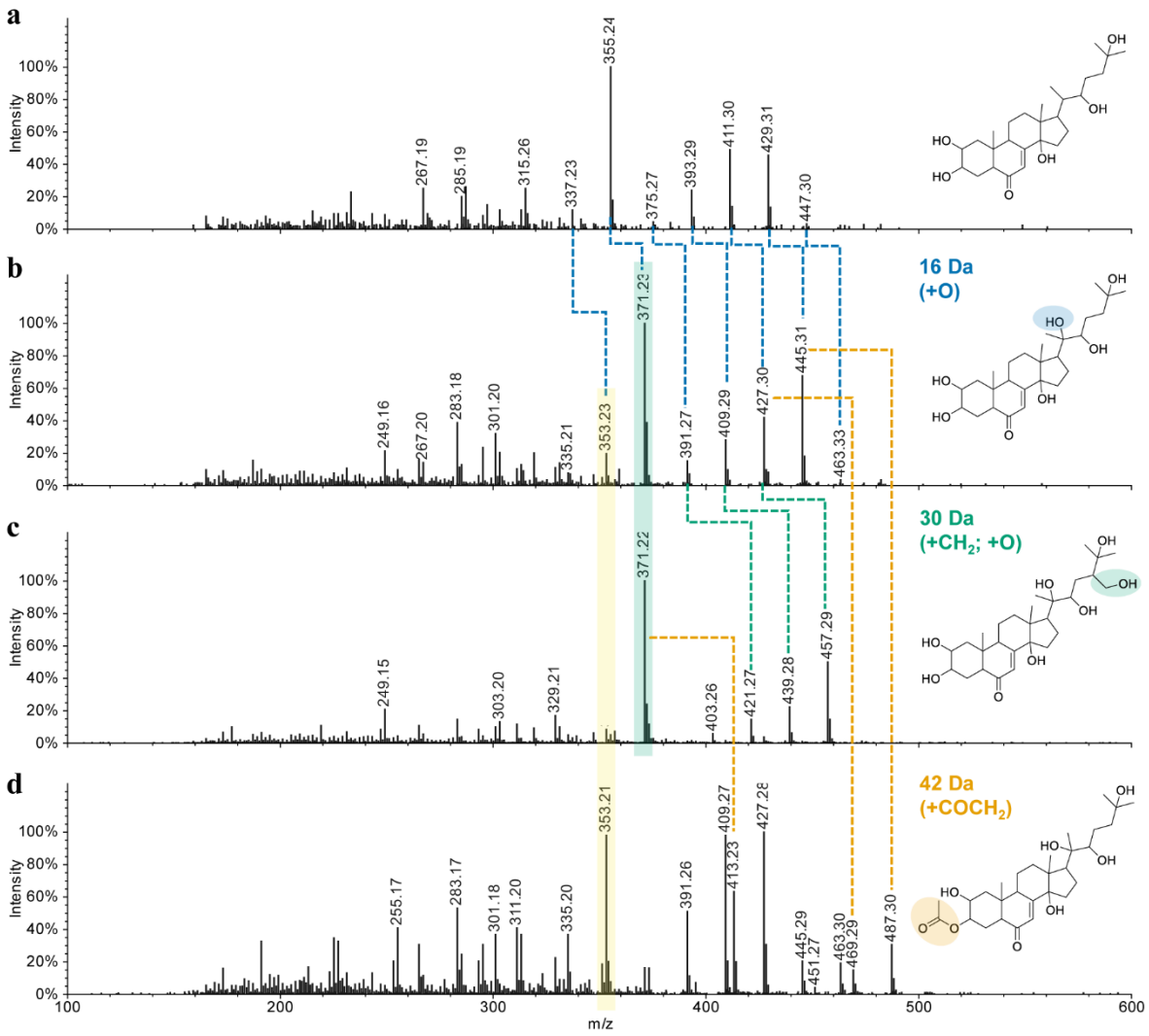

Figure 8S. *Comparative MS/MS spectra of ecdysteroid analogues showing diagnostic fragment ions and mass shifts. (a) Ecdysone; (b) hydroxyecdysone; (c) dihydroxymethylecdysone; (d) acetyl-hydroxyecdysone. Conserved fragment ions such as m/z 371 and 353 are shaded, indicating retention of core fragmentation across analogues. Colored dashed lines trace neutral losses consistent with functional group modifications on the side chain. Structures represent putative annotations based on spectral similarity and fragmentation pattern*

REFERENCES

1. Google Maps, https://maps.google.com/, accessed in July 2025.

2. Wang, M.; Carver, J. J.; Phelan, V. V.; Sanchez, L. M.; Garg, N.; Peng, Y.; Nguyen, D. D.; Watrous, J.; Kapono, C. A.; Luzzatto-Knaan, T.; Porto, C.; Bouslimani, A.; Melnik, A. V.; Meehan, M. J.; Liu, W. T.; Crüsemann, M.; Boudreau, P. D.; Esquenazi, E.; Sandoval-Calderón, M.; Kersten, R. D.; Pace, L. A.; Quinn, R. A.; Duncan, K. R.; Hsu, C. C.; Floros, D. J.; Gavilan, R. G.; Kleigrewe, K.; Northen, T.; Dutton, R. J.; Parrot, D.; Carlson, E. E.; Aigle, B.; Michelsen, C. F.; Jelsbak, L.; Sohlenkamp, C.; Pevzner, P.; Edlund, A.; McLean, J.; Piel, J.; Murphy, B. T.; Gerwick, L.; Liaw, C. C.; Yang, Y. L.; Humpf, H. U.; Maansson, M.; Keyzers, R. A.; Sims, A. C.; Johnson, A. R.; Sidebottom, A. M.; Sedio, B. E.; Klitgaard, A.; Larson, C. B.; Boya, C. A. P.;

Torres-Mendoza, D.; Gonzalez, D. J.; Silva, D. B.; Marques, L. M.; Demarque, D. P.; Pociute, E.; O'Neill, E. C.; Briand, E.; Helfrich, E. J. N.; Granatosky, E. A.; Glukhov, E.; Ryffel, F.; Houson, H.; Mohimani, H.; Kharbush, J. J.; Zeng, Y.; Vorholt, J. A.; Kurita, K. L.; Charusanti, P.; McPhail, K. L.; Nielsen, K. F.; Vuong, L.; Elfeki, M.; Traxler, M. F.; Engene, N.; Koyama, N.; Vining, O. B.; Baric, R.; Silva, R. R.; Mascuch, S. J.; Tomasi, S.; Jenkins, S.; Macherla, V.; Hoffman, T.; Agarwal, V.; Williams, P. G.; Dai, J.; Neupane, R.; Gurr, J.; Rodríguez, A. M. C.; Lamsa, A.; Zhang, C.; Dorrestein, K.; Duggan, B. M.; Almaliti, J.; Allard, P. M.; Phapale, P.; Nothias, L. F.; Alexandrov, T.; Litaudon, M.; Wolfender, J. L.; Kyle, J. E.; Metz, T. O.; Peryea, T.; Nguyen, D. T.; VanLeer, D.; Shinn, P.; Jadhav, A.; Müller, R.; Waters, K. M.; Shi, W.; Liu, X.; Zhang, L.; Knight, R.; Jensen, P. R.; Palsson, B.; Pogliano, K.; Linington, R. G.; Gutiérrez, M.; Lopes, N. P.; Gerwick, W. H.; Moore, B. S.; Dorrestein, P. C.; Bandeira, N.; *Nat. Biotechnol.* **2016**, *34*, 828 [Crossref]; Global Natural Products Social (GNPS), https://gnps.ucsd.edu, accessed in July 2025.

3. *SIRIUS*, version 6.1.0; Böcker, Germany, 2025.

4. GNPS spectral library, *CCMSLIB00010013013*, https://metabolomics-usi.gnps2.org/dashinterface/?usi1=mzspec%3AGNPS2%3ATASK-e3357317a6134042825c1fa21d0d6870-nf_output%2Fclustering%2Fspectra_reformatted.mgf%3Ascan%3A52&usi2=mzspec%3AGNPS%3AGNPS-LIBRARY%3Aaccession%3ACCMSLIB00010013013&width=6.0&height=4.0&mz_min=100.0&mz_max=400.0&max_intensity=199&annotate_precision=4&annotation_rotation=90&cosine=standard&fragment_mz_tolerance=0.1&grid=False&annotate_peaks=%5B%5B197.09469604492188%2C%20241.08309936523438%2C%20285.1424865722656%2C%20270.11981201171875%2C%20226.13380432128906%5D%2C%20%5B%5D%5D, accessed in July 2025.

5. GNPS spectral library, *CCMSLIB00011427929*, https://metabolomics-usi.gnps2.org/dashinterface/?usi1=mzspec%3AGNPS2%3ATASK-e3357317a6134042825c1fa21d0d6870-nf_output%2Fclustering%2Fspectra_reformatted.mgf%3Ascan%3A258&usi2=mzspec%3AGNPS%3AGNPS-LIBRARY%3Aaccession%3ACCMSLIB00011427929&width=6.0&height=4.0&mz_min=100.0&mz_max=500.0&max_intensity=199&annotate_precision=4&annotation_rotation=90&cosine=standard&fragment_mz_tolerance=0.1&grid=False&annotate_peaks=%5B%5B371.2226867675781%2C%20445.29620361328125%2C%20427.2853088378906%2C%20301.1831970214844%2C%20409.2755126953125%2C%20353.2109069824219%2C%20165.13470458984375%2C%20463.3055114746094%2C%20391.2638854980469%5D%2C%20%5B%5D%5D, accessed in July 2025.

6. GNPS spectral library, *CCMSLIB00011427929*, https://metabolomics-usi.gnps2.org/dashinterface/?usi1=mzspec%3AGNPS2%3ATASK-e3357317a6134042825c1fa21d0d6870-nf_output%2Fclustering%2Fspectra_reformatted.mgf%3Ascan%3A260&usi2=mzspec%3AGNPS%3AGNPS-LIBRARY%3Aaccession%3ACCMSLIB00011427929&width=6.0&height=4.0&mz_min=100.0&mz_max=500.0&max_intensity=199&annotate_precision=4&annotation_rotation=90&cosine=standard&fragment_mz_tolerance=0.1&grid=False&annotate_peaks=%5B%5B283.1827087402344%2C%20301.1954040527344%2C%20353.2254943847656%2C%20371.2348937988281%2C%20391.2680969238281%2C%20409.2947082519531%2C%20427.2976989746094%2C%20445.30810546875%2C%20463.3258972167969%2C%20165.1396026611328%5D%2C%20%5B%5D%5D, accessed in July 2025.

7. GNPS spectral library, *CCMSLIB00010086490*, https://metabolomics-usi.gnps2.org/dashinterface/?usi1=mzspec%3AGNPS2%3ATASK-e3357317a6134042825c1fa21d0d6870-nf_output%2Fclustering%2Fspectra_reformatted.mgf%3Ascan%3A1328&usi2=mzspec%3AGNPS%3AGNPS-LIBRARY%3Aaccession%3ACCMSLIB00010086490&width=6.0&height=4.0&mz_min=100.0&mz_max=500.0&max_intensity=199&annotate_precision=4&annotation_rotation=90&cosine=standard&fragment_mz_tolerance=0.1&grid=False&annotate_peaks=%5B%5B311.2580871582031%2C%20280.2608947753906%2C%20237.22970581054688%5D%2C%20%5B%5D%5D, accessed in July 2025.

8. GNPS spectral library, *CCMSLIB00010063486*, https://metabolomics-usi.gnps2.org/dashinterface/?usi1=mzspec%3AGNPS2%3ATASK-e3357317a6134042825c1fa21d0d6870-nf_output%2Fclustering%2Fspectra_reformatted.mgf%3Ascan%3A1441&usi2=mzspec%3AGNPS%3AGNPS-LIBRARY%3Aaccession%3ACCMSLIB00010063486&width=6.0&height=4.0&mz_min=100.0&mz_max=600.0&max_intensity=199&annotate_precision=4&annotation_rotation=90&cosine=standard&fragment_mz_tolerance=0.1&grid=False&annotate_peaks=%5B%5B184.08030700683594%2C%20313.2738952636719%2C%20496.3403015136719%2C%20478.3309020996094%2C%20258.1123962402344%5D%2C%20%5B%5D%5D, accessed in July 2025.

9. GNPS spectral library, *CCMSLIB00010058873*, https://metabolomics-usi.gnps2.org/dashinterface/?usi1=mzspec%3AGNPS2%3ATASK-e3357317a6134042825c1fa21d0d6870-nf_output%2Fclustering%2Fspectra_reformatted.mgf%3Ascan%3A1532&usi2=mzspec%3AGNPS%3AGNPS-LIBRARY%3Aaccession%3ACCMSLIB00010058873&width=6.0&height=4.0&mz_min=100.0&mz_max=600.0&max_intensity=199&annotate_precision=4&annotation_rotation=90&cosine=standard&fragment_mz_tolerance=0.1&grid=False&annotate_peaks=%5B%5B184.07919311523438%2C%20325.2803955078125%2C%20508.34161376953125%2C%20490.3319091796875%5D%2C%20%5B%5D%5D, accessed in July 2025.

10. GNPS spectral library, *CCMSLIB00010091229*, https://metabolomics-usi.gnps2.org/dashinterface/?usi1=mzspec%3AGNPS2%3ATASK-e3357317a6134042825c1fa21d0d6870-nf_output%2Fclustering%2Fspectra_reformatted.mgf%3Ascan%3A1621&usi2=mzspec%3AGNPS%3AGNPS-LIBRARY%3Aaccession%3ACCMSLIB00010091229&width=6.0&height=4.0&mz_min=100.0&mz_max=600.0&max_intensity=199&annotate_precision=4&annotation_rotation=90&cosine=standard&fragment_mz_tolerance=0.1&grid=False&annotate_peaks=%5B%5B184.0814971923828%2C%20339.2933044433594%2C%20308.2947998046875%2C%20265.25360107421875%5D%2C%20%5B%5D%5D, accessed in July 2025.

11. GNPS spectral library, *CCMSLIB00010064591*, https://metabolomics-usi.gnps2.org/dashinterface/?usi1=mzspec%3AGNPS2%3ATASK-e3357317a6134042825c1fa21d0d6870-nf_output%2Fclustering%2Fspectra_reformatted.mgf%3Ascan%3A1753&usi2=mzspec%3AGNPS%3AGNPS-LIBRARY%3Aaccession%3ACCMSLIB00010064591&width=6.0&height=4.0&mz_min=100.0&mz_max=600.0&max_intensity=199&annotate_precision=4&annotation_rotation=90&cosine=standard&fragment_mz_tolerance=0.1&grid=False&annotate_peaks=%5B%5B184.08009338378906%2C%20341.306884765625%2C%20524.3734741210938%2C%20506.3478088378906%2C%20258.1040954589844%5D%2C%20%5B%5D%5D, accessed in July 2025.

12. GNPS spectral library, *CCMSLIB00006678246*, https://metabolomics-usi.gnps2.org/dashinterface/?usi1=mzspec%3AGNPS2%3ATASK-e3357317a6134042825c1fa21d0d6870-nf_output%2Fclustering%2Fspectra_reformatted.mgf%3Ascan%3A2565&usi2=mzspec%3AGNPS%3AGN

PS-LIBRARY%3Aaccession%3ACCMSLIB00006678246&width=6.0&height=4.0&mz_min=100.0&mz_max=800.0&max_intensity=199&annotate_precision=4&annotation_rotation=90&cosine=standard&fragment_mz_tolerance=0.1&grid=False&annotate_peaks=%5B%5B259.202392578125%2C%20285.2412109375%2C%20333.24249267578125%2C%20543.4376220703125%5D%2C%20%5B%5D%5D, accessed in July 2025.

13. GNPS spectral library, *CCMSLIB00010057661*, https://metabolomics-usi.gnps2.org/dashinterface/?usi1=mzspec%3AGNPS2%3ATASK-e3357317a6134042825c1fa21d0d6870-nf_output%2Fclustering%2Fspectra_reformatted.mgf%3Ascan%3A2667&usi2=mzspec%3AGNPS%3AGNPS-LIBRARY%3Aaccession%3ACCMSLIB00010057661&width=6.0&height=4.0&mz_min=100.0&mz_max=800.0&max_intensity=199&annotate_precision=4&annotation_rotation=90&cosine=standard&fragment_mz_tolerance=0.1&grid=False&annotate_peaks=%5B%5B313.2723083496094%2C%20523.469482421875%2C%20285.2423095703125%5D%2C%20%5B%5D%5D, accessed in July 2025.

14. GNPS spectral library, CCMSLIB00006678245, https://metabolomics-usi.gnps2.org/dashinterface/?usi1=mzspec%3AGNPS2%3ATASK-e3357317a6134042825c1fa21d0d6870-nf_output%2Fclustering%2Fspectra_reformatted.mgf%3Ascan%3A2680&usi2=mzspec%3AGNPS%3AGNPS-LIBRARY%3Aaccession%3ACCMSLIB00006678245&width=6.0&height=4.0&mz_min=100.0&mz_max=800.0&max_intensity=199&annotate_precision=4&annotation_rotation=90&cosine=standard&fragment_mz_tolerance=0.1&grid=False&annotate_peaks=%5B%5B285.2424011230469%2C%20545.4547119140625%2C%20335.2579040527344%2C%20261.2203063964844%5D%2C%20%5B%5D%5D, accessed in July 2025.

15. GNPS spectral library, *CCMSLIB00006678247*, https://metabolomics-usi.gnps2.org/dashinterface/?usi1=mzspec%3AGNPS2%3ATASK-e3357317a6134042825c1fa21d0d6870-nf_output%2Fclustering%2Fspectra_reformatted.mgf%3Ascan%3A2742&usi2=mzspec%3AGNPS%3AGNPS-LIBRARY%3Aaccession%3ACCMSLIB00006678247&width=6.0&height=4.0&mz_min=100.0&mz_max=800.0&max_intensity=199&annotate_precision=4&annotation_rotation=90&cosine=standard&fragment_mz_tolerance=0.1&grid=False&annotate_peaks=%5B%5B285.24359130859375%2C%20521.4567260742188%2C%20311.2579040527344%5D%2C%20%5B%5D%5D, accessed in July 2025.

16. GNPS spectral library, *CCMSLIB00010013013*, https://metabolomics-usi.gnps2.org/dashinterface/?usi1=mzspec%3AGNPS2%3ATASK-e3357317a6134042825c1fa21d0d6870-nf_output%2Fclustering%2Fspectra_reformatted.mgf%3Ascan%3A2909&usi2=mzspec%3AGNPS%3AGNPS-LIBRARY%3Aaccession%3ACCMSLIB00000223895&width=6.0&height=4.0&mz_min=100.0&mz_max=600.0&max_intensity=199&annotate_precision=4&annotation_rotation=90&cosine=standard&fragment_mz_tolerance=0.1&grid=False&annotate_peaks=%5B%5B264.2681884765625%2C%20282.2792053222656%2C%20252.27000427246094%5D%2C%20%5B%5D%5D, accessed in July 2025.